TRANSACTIONS OF THE ASME

JOURNAL OF TURBOMACHINERY

PUBLISHED QUARTERLY BY ASME • JULY 2007

Engine Design Studies for a Silent Aircraft

Cesare A. Hall

Daniel Crichton

Department of Engineering,
Whittle Laboratory,
Madingley Road,
Cambridge, U.K

The Silent Aircraft Initiative is a research project funded by the Cambridge-MIT Institute aimed at reducing aircraft noise to the point where it is imperceptible in the urban environments around airports. The propulsion system being developed for this project has a thermodynamic cycle based on an ultrahigh bypass ratio turbofan combined with a variable area exhaust nozzle and an embedded installation. This cycle has been matched to the flight mission and thrust requirements of an all-lifting body airframe, and through precise scheduling of the variable exhaust nozzle, the engine operating conditions have been optimized for maximum thrust at top-of-climb, minimum fuel consumption during cruise, and minimum jet noise at low altitude. This paper proposes engine mechanical arrangements that can meet the cycle requirements and, when installed in an appropriate airframe, will be quiet relative to current turbofans. To reduce the engine weight, a system with a gearbox, or some other form of shaft speed reduction device, is proposed. This is combined with a low-speed fan and a turbine with high gap-chord spacing to further reduce turbomachinery source noise. An engine configuration with three fans driven by a single core is also presented, and this is expected to have further weight, fuel burn, and noise benefits. [DOI: 10.1115/1.2472398]

Introduction

The Silent Aircraft Initiative is a multidisciplinary project that is developing a concept aircraft with noise emission as the primary design driver. The aircraft is aimed at entry into service in about 20 years, and the ambitious objective is to reduce the noise generated to the point where it would be imperceptible above background noise in a typical urban environment outside an airport. Such an aircraft could be deemed as "silent," and this would represent a reduction in aircraft noise greater than that achieved over the last fifty years. Figure 1 illustrates the scale of this challenge, showing the Silent Aircraft noise target relative to the component noise levels for a current passenger aircraft. Note that to reach this noise level requires an aircraft that is less than half as noisy as the target identified by the ACARE vision for 2020 [1].

In order to reach the Silent Aircraft noise goal, large reductions, relative to current technology, are required for all components of engine and airframe noise. To make such large reductions, several methods must be employed simultaneously (see [2,3]). For example, to reduce jet noise, a very large, low-velocity exhaust flow is required combined with a power-management departure procedure. To make adequate turbomachinery noise reductions, the source noise can be reduced with improved component design and new engine configurations, but further attenuation of the noise is also needed using acoustic liners and shielding by the airframe [4].

In addition to the aggressive noise target, the new aircraft must be economical relative to other aircraft of the future. This requires a propulsion system that has competitive fuel burn as well as acceptable development, acquisition, and maintenance costs. Prior to the work in this paper, several trade studies were completed to determine the potential noise reductions possible for various engine configurations and to understand their implications for weight and performance [2]. This work found that a propulsion system embedded into the rear upper surface of an all-lifting body was best suited to meeting the project objectives. Furthermore, a turbofan system with a variable exhaust was shown to have the potential to have lower fuel consumption for a given noise level.

Several previous research projects have also studied advanced UHBR engine configurations aimed at significant improvements in noise and/or fuel consumption. For example, the NASA study of advanced engines for high efficiency [5] looked at several configurations, including geared fans and contra-fan designs, aimed at weight and fuel burn reductions. Another system study of engine concepts carried out by NASA [6] investigated the optimum engine parameters for low noise with acceptable operating costs. The design considerations for a new UHBR engine, aimed at reduced fuel burn, are clearly outlined in [7], and Ref. [8] gives a good overview of future technology required to further reduce noise from conventional aircraft engines. This proposes the use of geared turbofans to give a large improvement in noise emission.

A study of more radical propulsion concepts for a functionally silent aircraft is also presented in [9], which proposes distributed engine systems integrated with a blended-wing-body type aircraft.

What is new in the present study is that the off-design performance of the engine has been considered from the start of the design process. This is key since the engine conditions when low noise is essential are far from the design point (typically top-of-climb or cruise). In addition, the engine cycle in this project has been optimized for operation with a variable exhaust system and for an installation embedded within an all-lifting wing type airframe. Previous studies have tended to focus on engine designs intended for conventional tube-and-wing aircraft.

The current paper, therefore, aims to extend the previous work [2], which was based on quite simple analyses, to create more detailed designs of propulsion systems. In doing so, the off-design operation of a UHBR turbofan is examined and a design process for an advanced low-noise propulsion system is demonstrated. The designs are developed to the point where they can be assessed in terms of their performance, weight, and noise, and several possible engine arrangements are presented. Overall, this paper makes a contribution to the field of future engine designs for low noise and demonstrates the potential of UHBR engines with variable exhaust systems.

Propulsion System Requirements

The Silent Aircraft is expected to use an "all-lifting body" style of airframe [10]. The baseline design has a payload of 250 pas-

Contributed by the International Gas Turbine Institute of ASME for publication in the JOURNAL OF TURBOMACHINERY. Manuscript received July 13, 2006; final manuscript received July 23, 2006. Review conducted by David Wisler. Paper presented at the ASME Turbo Expo 2006: Land, Sea and Air (GT2006), Barcelona, Spain, May 8–11, 2006. Paper No. GT2006-90559

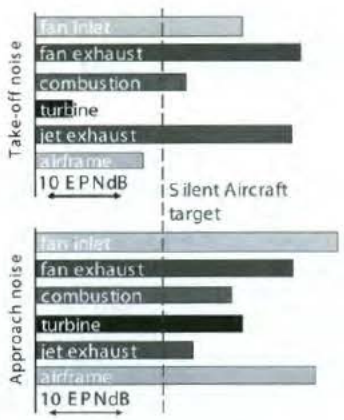

Fig. 1 Noise levels for a current 250 passenger aircraft compared with the Silent Aircraft target

sengers and a design range of 4000 nautical miles. This mission was chosen to give the lowest weight aircraft that would be economically competitive with other civil airlines. A 3-D view of a CAD representation of a possible airframe and propulsion system is shown in Fig. 2.

Studies with an airframe design tool were used to determine the thrust requirements at different points in the mission with corresponding altitudes and Mach numbers. The flight mission profile was chosen to give the lowest aircraft take-off weight (MTOW), with the assumption that this would minimize the noise radiated at take-off and approach. The methodology and analysis used to optimize the airframe design is described in detail within [12]. Table 1 summarizes the resulting requirements of the propulsion system at key operating conditions in the flight envelope.

For the purposes of this paper, the noise target of the Silent Aircraft is expressed as a peak dBA value that cannot be exceeded at any point on the ground outside the airport boundary during take-off and landing in normal operating conditions. This peak dBA limit was imposed because this can be linked to both World Health Organization guidelines on community noise and data on average traffic noise levels in urban areas [13,14]. Normal operating conditions are taken as an atmospheric temperature of below ISA+12 K and a runway length of 3000 m. This allows the aircraft to operate in a "nonsilent" mode for any remaining extreme conditions ("short & steep," "very hot," and "hot & high" take-off).

Fig. 2 A 3-D rendering of a candidate Silent Aircraft airframe and propulsion system, taken from [11]

Table 1 Propulsion system mission requirements

Condition	Altitude (m)	Mach number	Total thrust (kN)	SFC (g/sN)	Noise target (peak dBA)
Sideline	180	0.23	316.8	—	<57.0
Flyover	195	0.24	172.8	—	<57.0
Top-of-climb	12,192	0.80	82.4	—	—
Mid cruise	12,570	0.80	65.4	<15.0	—
Approach	120	0.23	<72.0	—	<57.0

For take-off, an optimized departure profile was used in which the thrust was managed to achieve the maximum climb rate without exceeding the noise target in terms of jet noise. This procedure is demonstrated in [3], and it was found that a total exhaust area of 13.2 m^2 would be required to enable an acceptable departure profile. The sideline and flyover conditions represent two points in the departure profile that are critical in terms of noise. At sideline, the aircraft is still inside the airport boundary and the climb rate is highest. At flyover, the aircraft is closest to the population on the ground. The sideline lateral position is the same as the ICAO certification distance of 450 m, but the flyover point used is closer to the runway (4048 m rather than 6500 m after brakes off).

Top-of-climb (TOC) is the condition that determines the size of the engine. This is where high thrust is required to keep climbing and the atmosphere is thin. For an economically viable aircraft of the future, the installed engine specific fuel consumption (SFC) at cruise was specified to be at least as competitive with the next generation high bypass ratio podded turbofan engines (15 g/sN =0.53 lb/lbh). Note that improvements in SFC are beneficial in terms of total noise because they reduce the weight of fuel that needs to be carried, and thus the MTOW.

For the approach condition, a maximum net thrust target was specified in order to limit the airframe drag required. A greater drag leads to higher airframe noise through the dissipation of turbulent kinetic energy in the wake. The minimum thrust specified was chosen to be as low as possible while enabling an engine spool-up time (the time required for the engine to accelerate to maximum thrust) that would be comparable to current turbofans.

Note that all the engine design studies in this paper are matched to the same all-lifting body airframe and flight mission. The methodology applied to develop the engine cycle and the mechanical designs should be equally applicable to the propulsion systems for other airframe configurations. However, a different airframe or installation would have a large impact on the values of many of the engine characteristics.

Engine Installation Considerations

Before the parameters of the engine cycle can be specified some characteristics of how the propulsion system is packaged with the airframe need to be considered. For the Silent Aircraft design, the engines are positioned on the upper surface of the airframe, towards the trailing edge (as illustrated in Fig. 2). This location was adopted to take advantage of the performance benefits of boundary layer ingestion and to maximize the shielding of forward arc engine noise [4]. It also offers airframe control and safety advantages, because the engines are positioned well behind the passenger bays [12].

A target S-shaped inlet performance was assumed based on results in the open literature; for example [15,16], and preliminary CFD studies [17]. Several calculations were completed at the cruise condition for different numbers of engines and various intake configurations. The current baseline design has 4 separate engine units (Fig. 2), which gives an acceptable fan diameter and good installation performance. The mesh geometry and Mach number contours, from a calculation of this configuration, are as shown in Figs. 3 and 4, respectively. Figure 4 shows how a large region of high loss flow builds up at the bottom of the inlet duct as the engine face is approached, and this is typical for an S-shaped duct.

The final propulsion system for the Silent Aircraft is expected to use boundary layer ingestion (BLI) to give a fuel burn benefit, as mentioned above, and as discussed in [2]. BLI introduces significant challenges to both the engine and airframe design. In particular, BLI generates additional nonuniform flow distortion in both the radial and circumferential directions, which is present at

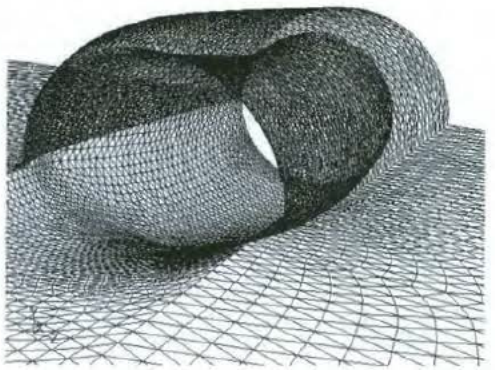

Fig. 3 View of the surface mesh for a four-engine installation, taken from [17]

all flight conditions. BLI also changes the engine thrust requirements because any boundary layer fluid that passes through the engine and contributes to thrust would have otherwise contributed to airframe drag. Thus, to progress the engine design for the studies in this paper, the engine inlets were temporarily assumed to be boundary layer diverting (BLD). This enables the engine thrust requirements to stay as per Table 1. The impact of BLI on the engine performance and the airframe requirements will be included in future work.

CFD results for S-shaped inlet ducts all show significant separated regions at the fan-face. From the inlet highlight to the fan-face, a typical S-shaped inlet was found to have a pressure recovery (p_{02}/p_{01}) of about 0.96. This value can be applied to both BLI and BLD cases, and it was used in the following engine design studies as a target performance for the engine inlet. Overall, it is expected to be a lower-bound estimate because design improvements and flow control should be able to reduce the losses. The level of circumferential distortion was also determined from the predictions, and in terms of DC60 (an industry measure of the severity of flow nonuniformity), the S-duct gave values of around 20%. The impact of this distortion on the system design will be explored in detail in future research, because it is mainly a consequence of BLI. The designs presented in this paper are therefore intended to tolerate this level of distortion, but are not optimized for performance with it present.

The engine exhaust is considered as a long cylindrical duct in which the core and bypass streams are mixed completely, followed by a loss-free variable nozzle. The exhaust duct pressure losses were determined using simple compressible pipe flow analysis (Fanno line flow) with skin friction coefficients appropriate for the surface of a perforated acoustic liner. The exhaust duct size was set to match the maximum nozzle area required for a quiet take-off. This size of duct was used to avoid a "diffusing nozzle" being necessary at any point in the aircraft flight envelope. The length of mixer duct was set at 2 fan diameters to accommodate a large area of downstream acoustic liners. This led to an exhaust pressure recovery (p_{08}/p_{064}) of 0.98 for the designs in this paper.

Fig. 4 Contours of Mach number through a four-engine installation, taken from [17]

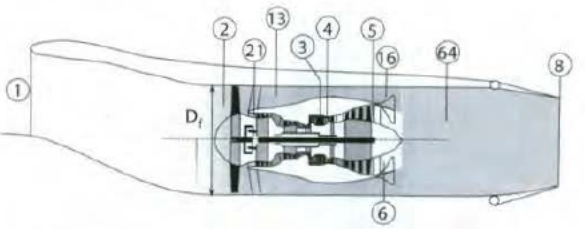

Fig. 5 Schematic of engine layout showing station numbering, adapted from [18]

Engine Cycle Design

The engine configurations developed in this paper are ultrahigh bypass ratio (UHBR) turbofans combined with variable area exhaust nozzles. This configuration was identified in [2], and for the aircraft mission requirements it was expected to be more suitable than other possible variable cycle systems such as bypass stream ejectors or a system with auxiliary fans. The optimum solution for a different mission requirement may be quite different. The engine station numbering used for the thermodynamic cycle is as shown in Fig. 5.

To allow for technological advances, 2025 estimates of peak component efficiencies and metallurgical limits were made by extrapolating historical trends. These were imposed as limits on the engine cycle temperatures and component efficiencies that could not be exceeded at any point in the engine operation. It was expected that a future quiet engine would have a similar maximum fan capacity to today's turbofan designs, but that this could be achieved at a lower fan pressure ratio and tip speed (see [2]). A maximum fan capacity was therefore imposed as a constraint and combined with a generic low pressure ratio fan characteristic to estimate off-design performance variations. It was also predicted that advances in mechanical properties would allow the hub-to-tip radius ratio of a future fan to be lower than current designs. A value of 0.25 was used to minimize the fan diameter (current designs are typically in the range 0.3–0.35).

In order to develop an engine cycle, a design condition is chosen to fix the engine size and key parameters. For this study, the top-of-climb point was used and the thermodynamic cycle was optimized to minimize the fan diameter and fuel consumption at this condition. The top-of-climb point was then considered with the other off-design conditions and some iteration was employed to optimize the performance for every engine operating condition in Table 1.

Cycle Optimization at Top-of-Climb. The engine design cycle was developed using GasTurb10 [18] with the aim of producing the most compact and fuel-efficient engine that would satisfy the requirements in Table 1. Figure 6 shows how an engine cycle appropriate for the future Silent Aircraft was evolved from a current conventional turbofan. Each bar in the figure represents a redesign of the engine in which the fuel consumption has been minimized and the net thrust and temperature limits have been constrained. The relative heights of the adjacent bars show the impact of each design change on engine fuel consumption and engine size. The aim of such a chart is to show that the final

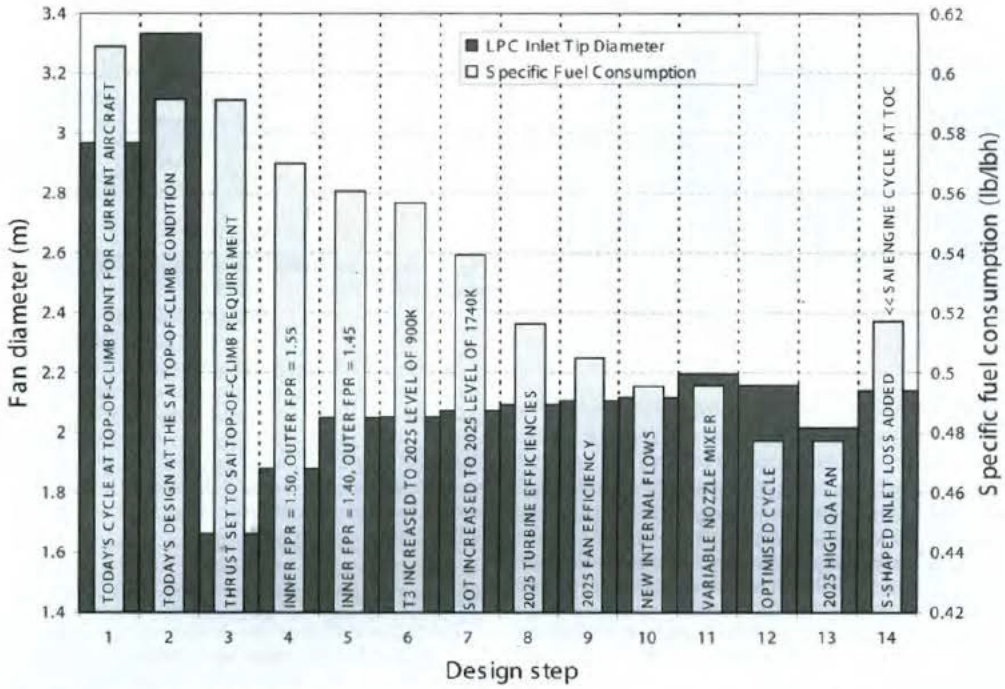

Fig. 6 Evolution of the Silent Aircraft engine cycle at top-of-climb assuming a four-engine system

design cycle is feasible. The changes in the height of the bars between each design show the incremental effects of changing the design cycle parameters.

The first three steps shown in Fig. 6 represent the design changes necessary to match today's turbofan engine to the top-of-climb condition in Table 1. The two subsequent changes indicate how a large performance benefit can be attributed to the low fan pressure ratio that is specified (steps 4 and 5). A drawback of this is that the fan diameter increases significantly as FPR is reduced. Higher temperature limits and improved turbine performance contribute significantly to improving core efficiency (steps 6, 7, and 8). However, as the engine efficiency is improved, the fan diameter has to increase to maintain the same net thrust. This effect is also seen when the fan efficiency is increased and the losses due to internal air systems are reduced (steps 9 and 10). The exhaust duct that is specified is larger than optimum to match the variable area nozzle (step 11) and this also leads to a slightly larger fan. The cycle was then optimized for best thermodynamic performance (step 12). This involved iterating to determine the bypass-to-core total pressure ratio (p_{016}/p_{06}) that gave the minimum SFC. The use of the high capacity, low hub-tip-ratio fan (step 13) gives further improvements. However, the introduction of the S-duct inlet total pressure loss (step 14) increases the fan diameter and significantly worsens the overall performance.

Note that the design cycle used in this paper has a fan pressure ratio of 1.45, and for a four-engine case, a fan diameter of 2.16 m. The choice of design FPR is a compromise that is driven by several factors. A lower value leads to higher propulsive efficiency at the cost of a larger engine size, which increases the total installed drag. In terms of noise, as FPR reduces it becomes easier to meet the jet noise target, and the nozzle area change needed between take-off and top-of-climb is minimized [19]. Fan source noise also tends to reduce with FPR, as shown later in this paper in Fig. 14. Unfortunately, a lower FPR design is heavier and more sensitive to inlet distortion and to installation pressure losses, as shown in [2].

A top-of-climb FPR of 1.45 was therefore chosen as the lowest possible value that would be achievable with a robust mechanical design. The corresponding engine bypass ratio is 15.5, which clearly makes it a UHBR. However, BPR is not a good design parameter to characterize the engine because it changes significantly between operating conditions (see Table 2, later). The SFC at top-of-climb is 14.7 g/sN, which is slightly better than the best turbofans operating today. This seems realistic for a UHBR engine in 2025 within an S-type inlet.

Off-Design Operation. Using the final cycle design developed above, the engine parameters at other points in the flight mission were determined. With the engine size fixed and the thrust constrained, the main degree of freedom available is the nozzle setting. At each of the flight conditions in Table 1, the fan can operate anywhere along a characteristic of constant thrust. Figure 7 shows scaled constant-speed fan characteristics based on [20] with constant-thrust characteristics overlaid (dashed) for each of the key operating conditions. The optimum operating points used for the final design are marked as small circles. The precise perfor-

Table 2 Cycle parameters for the Silent Aircraft engine design in this paper

Parameter	Sideline	Top-of-climb	Cruise	Unit
FPR	1.27	1.45	1.40	—
$N_f/\sqrt{T_{02}}$	90	100	99	%
ΔA_8	+35	0	+8	%
M_{a2}	0.64	0.66	0.70	—
η_{fan}	94.5	90.4	93.4	%
T_{03}	910	900	840	K
T_{04} (TET)	1730	1880	1700	K
OPR	41.0	57.4	53.9	—
BPR	19.0	15.5	16.8	—
SFC	8.8	14.7	14.2	g/sN

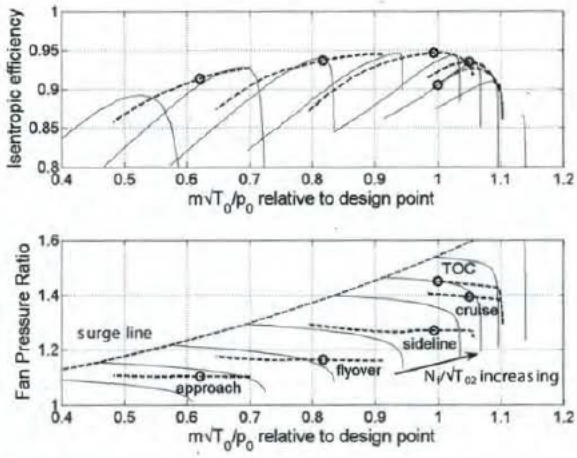

Fig. 7 Operation of the Silent Aircraft engine fan for a variable nozzle design

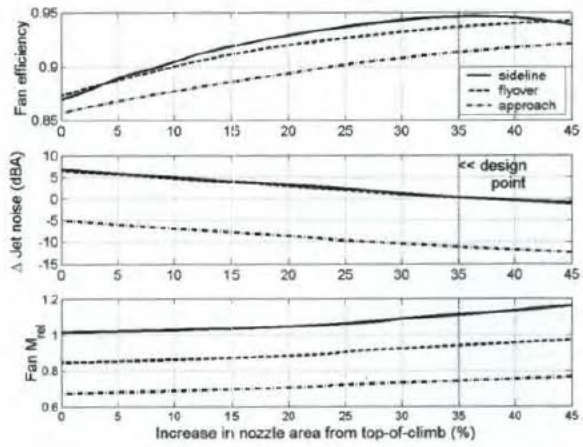

Fig. 9 Variation in fan efficiency, jet noise, and fan tip relative Mach number with nozzle area.

mance depends on the shapes of the fan characteristics, so these plots can be viewed as an example case. Improved fan characteristics for a full 3-D fan design are developed in the companion paper [19].

The characteristics in Fig. 7 have been scaled around the design FPR of 1.45 (top-of-climb) and a peak rotor isentropic efficiency of 94.5% (the maximum possible expected in 2025). By varying the nozzle exit area while maintaining the net thrust constant-thrust lines could be produced. These were further constrained by shaft speed and temperature limits. The optimum top-of-climb point is positioned towards the stability margin on the 100% speed characteristic. This was done primarily so that the exhaust nozzle could be opened sufficiently at sideline to give higher fan capacity at this condition (and thus low jet noise), while keeping high efficiency. The design condition can be positioned further down the maximum speed characteristic, but this reduces the operating range available at other conditions. The fan capacity at cruise is allowed to increase slightly without exceeding the design fan shaft speed to give improved efficiency.

Figure 8 shows the fan characteristics if the same mission requirements and design engine cycle are assumed for a fixed nozzle

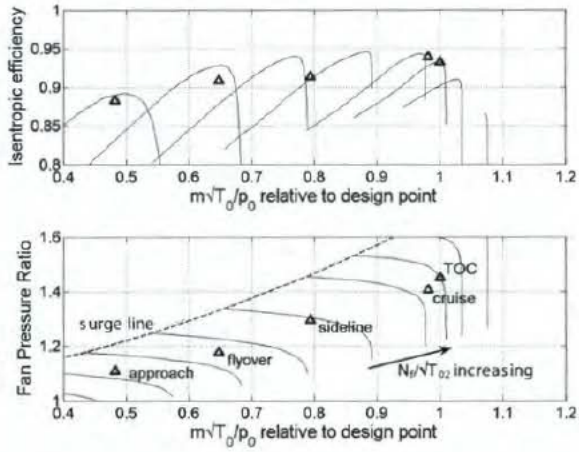

Fig. 8 Operation of the Silent Aircraft engine fan for a fixed nozzle design

engine. In this case, the fan is constrained to work at a single working point for each flight condition. The top-of-climb point is positioned so that the cruise condition is at peak efficiency. The sideline, flyover, and approach points are thus fixed at lower flow rates, which are at higher fan pressure ratios and closer to instability than for the case with a variable nozzle.

Table 2 details the key cycle parameters at sideline, top-of-climb, and cruise corresponding to the operating points in Fig. 7. This illustrates the component performances and the cycle temperatures that are required to achieve the design requirements. It is important to emphasize that the operation of the Silent Aircraft engine with a variable area nozzle differs significantly from that of an engine with a fixed nozzle operated for a conventional aircraft. Firstly, the fan pressure ratio at take-off is much lower than at cruise or top-of-climb. The principal reason is that only a fraction of the available thrust at take-off is needed. The total sea level static thrust available from the propulsion system (all engines) is about 570 kN, and less than 60% of this is needed at the sideline condition. The low thrust requirement at sideline is key to minimizing the jet noise, and this is further exploited with an optimized take-off procedure that is described in [3].

Another unusual aspect of the design is that the fan speed is similar at all the three conditions in Table 2, and the fan-face Mach number is consistently high. Previous studies [2] showed that a high fan capacity at take-off leads to lower jet noise and Figs. 7 and 9 demonstrate how this can be achieved with a variable exhaust nozzle.

The variations in cycle temperatures and pressures are also different from a conventional turbofan. Usually the cycle temperatures are all highest at take-off, and it is this condition that is most demanding in terms of the mechanical stresses. For the design developed here the compressor outlet temperature is highest at take-off, but only slightly above the top-of climb and cruise points. The turbine entry temperature is a maximum at top-of-climb, where the overall pressure ratio is also much greater than the sideline condition. This occurs because the thrust requirement of the engine during take-off is only a fraction of the total thrust available.

The variable nozzle has the potential to reduce fuel consumption. It should be possible to carefully control the nozzle position to maximize the fan efficiency at all flight conditions, as indicated in Fig. 7. For a fixed nozzle design, a fan is constrained to operate on a working line that might not be at peak efficiency. In addition, the fan characteristics of an engine operating in-service may not be exactly as predicted. A variable nozzle enables performance discrepancies to be corrected during flight, ensuring the optimum

Table 3 Principal mechanical parameters for the engine designs presented

	Design A	Design B	Design C	Design D
Configuration	Three-spool turbofan	Two-spool geared fan	Two-spool, slower fan	Multiple fan system
D_f (m)	2.16	2.16	2.18	1.28
l_{eng} (m)	3.46	2.42	2.70	2.70
n_{eng}	4	4	4	12
Number of fan rotor blades	20	20	18	18
Max. U_{tip} (m/s)	380	380	350	350
IPC/booster stages	7	7	8	8
HPC stages	10	5	5	5
HPC min. blade height (mm)	10	22	22	22
LP turbine stages	9	4	4	4
W_{eng} (%)	100	99.2	91.4	81.3

efficiency is achieved.

A variable exhaust nozzle can also improve the engine operability. During take-off, with the nozzle fully opened, the fan operates well away from the stability line. This is particularly helpful for a low FPR fan at this point in the flight mission because the engine is at risk of crosswind induced inlet separation. A carefully controlled variable nozzle could enable other aeromechanical problems such as flutter to be avoided at other key conditions in the flight envelope.

The variations in fan efficiency, tip relative Mach number, and exhaust jet noise (relative to the target level), along the constant-thrust characteristics in Fig. 7, are shown in Fig. 9 for the three noise critical operating conditions. A design fan tip speed of 350 m/s (at top-of-climb) has been assumed for this figure. The plots illustrate that as the exhaust nozzle is opened, the performance of the fan is improved. The jet noise, as computed using the Stone jet noise model [21], decreases as the nozzle is opened because the jet velocity reduces substantially. However, the fan tip speed and axial flow velocity have to increase to maintain the same thrust. Fan broadband noise is typically correlated against tip relative Mach number (ESDU 98080, [22]) and other fan noise sources increase with tip speed. Thus, there is a trade-off between fan source noise and jet noise, which demands careful attention. This aspect is explored further in the companion paper [19], which shows that by positioning the fan operating condition at a point of high efficiency during take-off, it is possible to reduce fan source noise while still meeting the jet noise target.

Preliminary Engine Mechanical Designs

A preliminary mechanical design system provided by Rolls-Royce plc was used to create engine architectures that could achieve the engine thermodynamic cycle detailed in the previous section. A mechanical design is driven by the flight condition where the engine temperatures and pressures are highest because this creates the highest stresses. However, the component designs must also satisfy the aerodynamic loadings required at all points in the flight envelope. For the Silent Aircraft engine, a maximum sea level thrust condition was used to create the most mechanically demanding condition, and this was combined with the top-of-climb point for the peak aerodynamic loadings and peak non-dimensional flow rates.

To complete a mechanical design, the cycle conditions are input and these are combined with design rules for each of the engine components: fan, compressors, combustor, turbines, ducts, shafts, and bearings. The rules applied specify geometric, stress, and aerodynamic limits that are used to determine an acceptable engine layout. Within the software it is possible to vary the engine components that are included within the engine design and also to modify how they are linked together.

Table 3 summarizes the parameters of the four engine designs presented in this paper. All the configurations satisfy the cycle parameters shown in Table 2 and the mission requirements in Table 1.

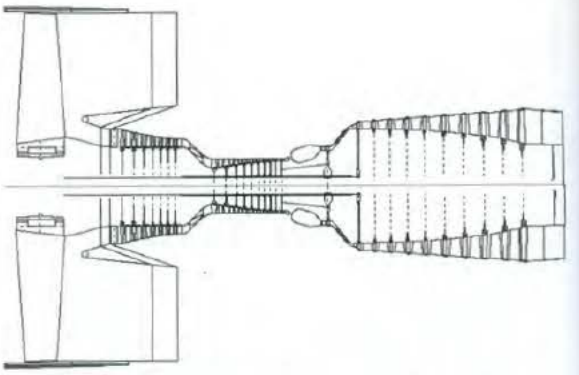

Fig. 10 Design A: 3-spool conventional turbofan design for the Silent Aircraft

Design A is a conventional three-shaft turbofan architecture. The general arrangement for this design (Fig. 10) was obtained using current design levels of aerodynamic loading and stress, and typical geometrical constraints for the turbomachinery annulus. There are several problems with this design that make it an unrealistic solution. Firstly, the LP turbine has nine stages, making it very bulky, heavy, and noisy. This is necessary in order to drive the relatively large fan at low rotational speed. The low shaft speed also leads to high torque, demanding very thick shafts. The core annulus is quite convoluted and S-ducts with dramatic changes in radius between the IP and HP turbines are required. Ten stages of HP compressor are required to achieve the cycle OPR and this demands a blade height in the final stage of less than 10 mm. This size of blade would suffer significant losses from Reynolds number effects and tip clearance flows, and it would be very difficult to manufacture accurately with current tools.

Design B, illustrated in Fig. 11, was developed in order to address the problems identified in Design A. To reduce the LP turbine size a 3:1 reduction gearbox has been placed between the fan

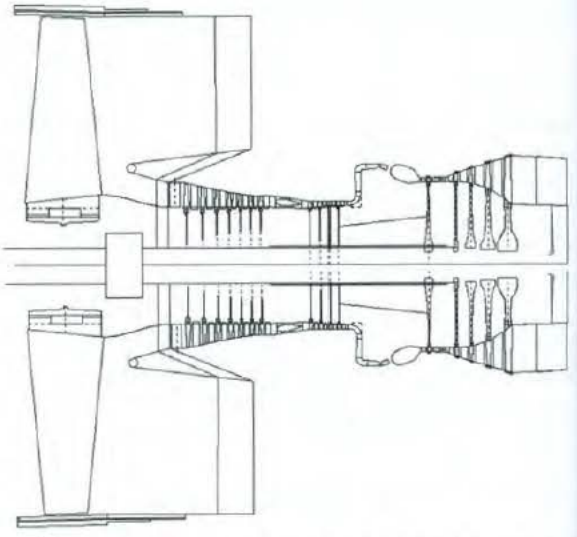

Fig. 11 Design B: Geared turbofan for the Silent Aircraft with axial-radial HP compressor

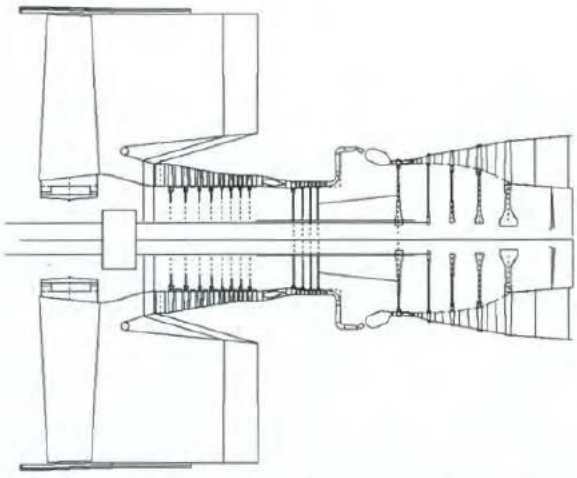

Fig. 12 Design C: Geared turbofan for the Silent Aircraft modified for lower noise

and compressor. The engine is thus a two-shaft design with what previously were the IP compressor (now booster) and the IP turbine all on the same LP shaft and spinning at three times the speed of the fan. The torque in the LP shaft is therefore reduced and the stage loadings in the LP turbine are kept at an acceptable level, despite there only being four stages driving both the fan and booster compressor. The gearbox weight for this engine was estimated as 8% of the total engine weight, which is significant, but much smaller than the weight of the original LP turbine. However, the engine weight is not greatly reduced from that of Design A because of the introduction of a heavy centrifugal HP compressor stage. This was added to remove the S-shaped ducts in the annulus and to increase the minimum blade height in the HP compressor, thus making the engine easier to manufacture. Overall, the engine is much more compact and it appears to be more viable than Design A. However, it had not been optimized for low noise, and initial estimates predicted that the source noise levels from this design would be too high.

Design C (Fig. 12) was created as a quieter and lighter version of Design B. The main changes were to reduce the fan tip speed and to increase gap-to-chord ratios in the turbine. All sources of fan noise tend to increase with fan tip speed. Supersonic noise sources also appear if the relative blade Mach number exceeds unity. The control of blade tip speed for minimum noise is explored further in the companion paper [19]. For the purposes of this paper, it was assumed that the aerodynamic loading of the fan could be significantly increased without reducing the efficiency. The fan in Design C therefore has a design tip speed of 350 m/s with only 18 rotors. If the same 3:1 gearbox is assumed, the loadings on the LP turbine and booster compressor increase leading to more aerofoils and an extra stage of compressor.

To minimize the turbine source noise during approach the gap-to-chord ratios in all stages of the LP turbine were increased to above 100%, whereas in Design B the spacing was as small as possible for low weight and size. Despite Design C being larger than Design B, the overall weight of the fan system and the containment is reduced significantly, giving a reduction in the total bare engine weight of about 8%.

Design D is shown in Fig. 13. It was developed to study the effects of having multiple fans driven by a single core, which is a configuration expected to give noise and fuel consumption benefits. In this case there would be a total of 12 fans and 4 engine cores in the propulsion system. Although this is a radically different approach to the previous designs, it still satisfies the same engine cycle and mission requirements. The core design is identical to Design C. Each of the fans also has the same hub-tip ratio as the previous designs and the overall mass flow rates are identical. The results from the design tool show that Design D is 11% lighter than Design C in terms of bare engine weight (Table 2). A formula relating engine weight to fan diameter is proposed in [2] (eq. (11)), which would suggest a weight reduction closer to 20%. However, the actual change is expected to be smaller because only the fan system weight is reduced, rather than scaling all components down, which is assumed in [2].

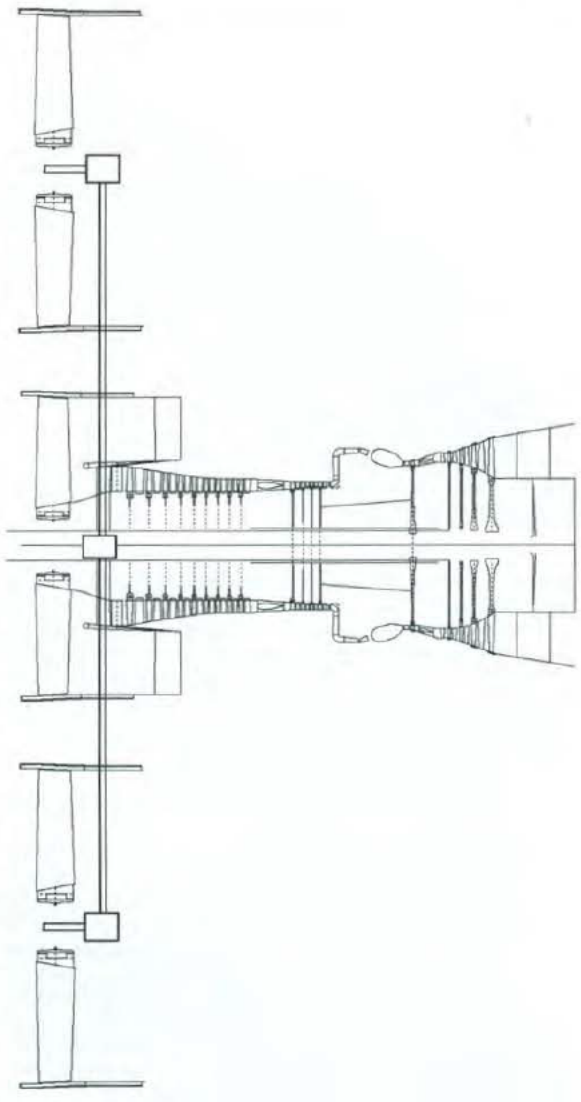

Fig. 13 Design D: Multiple fan version of a geared turbofan for the Silent Aircraft

The layout of Design D is thought to have two advantages in terms of noise. Firstly, the length-to-diameter ratio of the exhaust ducts can be extended to increase the attenuation from acoustic liners [2]. Secondly, if the fan tip speed is maintained, as has been done in this design, the fan shaft speed must increase, and therefore the blade passing frequency increases. Higher frequencies are more readily attenuated by liners and are more effectively shielded by the airframe [4], leading to lower noise transmission. Design D is also expected to have potential fuel burn benefits

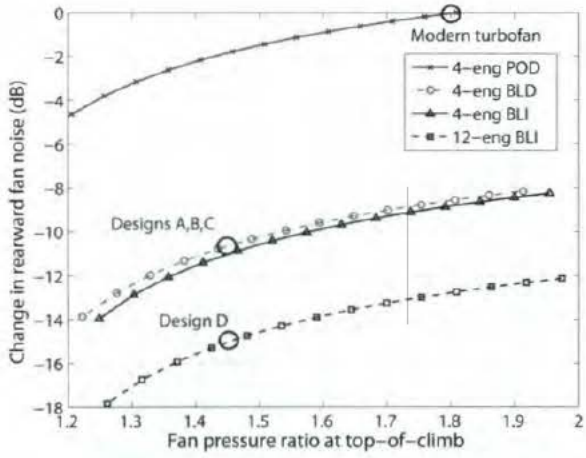

Fig. 14 Variation in rearward fan noise with design fan pressure ratio based on ESDU 98008 [22]

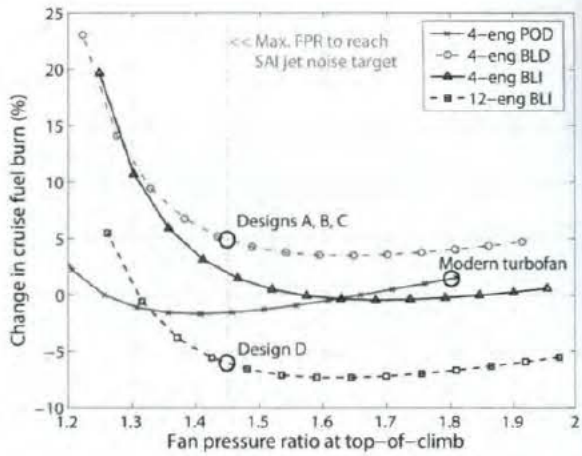

Fig. 15 Variation in cruise fuel burn with design fan pressure ratio and installation configuration

because it enables the propulsion system to be better packaged into the airframe, reducing the installation drag contribution and also increasing the total amount of airframe boundary layer that can be swallowed by the engine inlets [2]. These effects on noise and fuel consumption are explored further in the section below. The added mechanical complexity of the additional shafts and gearboxes required for this design is not considered further here, although this is expected to create additional design challenges. There are also safety issues, such as the greater risk of containment failures impacting on adjacent systems, which also need to be accounted for.

Installation Trade Studies. A simple analysis is presented in [2] that allows different engine configurations to be readily compared in terms of noise, weight, and fuel consumption. This section applies a similar analysis to examine the relative merits of the different engine designs presented and to see how noise and fuel burn would change were a different design FPR value chosen.

Using the thrust requirements at take-off and top-of-climb, once the installation configuration is fixed, the fan diameter and the exhaust flow conditions can be determined for a given design FPR. This enables variations in jet and fan noise to be estimated from correlations such as those in [21,22]. Figure 14 shows the expected trends in rearward fan broadband noise for different possible installation options. The changes are shown relative to a reference level, which is the noise from a two-engine podded turbofan propulsion system with a design FPR typical of today's technology. This reference level was chosen because it is representative of a current conventional design.

Each of the configurations considered in the plots satisfies the mission requirements in Table 1, and in all cases a variable exhaust nozzle is assumed in which the fan capacities at top-of-climb and sideline are matched. Podded, BLD, and BLI cases are included in order to show the expected improvement in noise reduction from a longer installation. The plots indicate how fan noise reduces continuously with design FPR. This occurs because at a fixed thrust level, design fan tip speed reduces to maintain the same aerodynamic stage loading. This effect outweighs the increase in noise caused by the increased fan diameter. The results suggest that Design D, with exhaust ducts of a high length-to-diameter ratio, will be much quieter than a podded equivalent and a few dB quieter than the equivalent four-engine embedded system.

The fuel burn effects of different installation options were explored with a similar trade study. The results are shown in Fig. 15, which shows fuel burn variation relative to a two-engine podded turbofan propulsion system with a design FPR typical of today's technology. The analysis includes several factors that are calculated using the formulae in [2]: (i) the increase of wetted area drag with engine size, (ii) the increase in propulsive efficiency with reduced jet velocity, (iii) the reduction in overall efficiency with losses in the intake and exhaust, and (iv) the drag reduction of the airframe produced by boundary layer ingestion. Again, the aircraft mission requirements in Table 1 were used, and all the engines were assumed to be turbofans fitted with a variable area exhaust nozzle in which the values of fan capacity at take-off and top-of-climb were matched to the design value. For the embedded configurations, the installation pressure recovery factors were the same as used for the engine cycle design described previously. With BLI, an extra inlet total pressure loss of 2% was included to account for the lower total pressure of the ingested boundary layer flow.

Note that the SFC values calculated for the engine cycle design study (Table 2) do not account for differences in installation drag. Furthermore, SFC cannot be used to follow the effects of boundary layer ingestion, and therefore the rate of fuel consumption is a better measure of overall performance.

Figure 15 shows that there is an optimum design FPR in terms of fuel burn, which differs depending on the type of installation and the number of engines. Although the podded design is found to have greater installation drag, it benefits from having a simple inlet and a short exhaust with low total pressure losses. Thus, the lowest fuel burn occurs at a low design FPR and thus at a high fan diameter. The fans in the embedded systems (BLI and BLD) are very susceptible to installation duct losses, and the effect of these is larger at low fan pressure ratios. This leads to higher fan pressure ratios being preferable for embedded systems. However, as shown by Fig. 14 and the studies described in [19], as fan pressure ratio increases, the jet and fan source noise will increase.

This study shows that Design D, at a design fan pressure ratio of 1.45, could offer a potential 12% reduction in fuel consumption relative to a four-engine system without boundary layer ingestion. Relative to a podded design, the fuel burn benefit is lower, around 5%. If a higher design FPR could be used the benefit of BLI could be greater. This may make the jet noise target more difficult to reach, but as indicated by Fig. 14, an embedded propulsion system with multiple ducts should be quieter in terms of turbomachinery noise.

Conclusions

An optimized cycle for an embedded UHBR turbofan operating with a variable exhaust nozzle has been devised. Realistic estimates of the performance of an S-type inlet and the technological limits in 2025 have been included, and these lead to a feasible thermodynamic cycle for the Silent Aircraft propulsion system. The cycle used as a basis of further design studies has a top-of-climb fan pressure ratio of 1.45.

The off-design operation of a UHBR turbofan with a variable exhaust nozzle can be optimized for low noise, during approach and take-off, and for performance at cruise. The benefits relative to a fixed nozzle design have been demonstrated and the engine cycle variations for the Silent Aircraft design have been determined. For the design study described in this paper, the nozzle required has a maximum area variation of 35%. This enables the jet noise target to be reached and also improves the fan efficiency and stability margin during take-off.

Preliminary mechanical designs have been completed for the Silent Aircraft engine thermodynamic cycle. A two-spool geared turbofan with a gearbox between the fan and booster compressor and an axial-radial HP compressor gives a compact, low-weight design. This has been modified by reducing the fan tip speed and by increasing the turbine spacing; this is expected to lower component source noise, while further reducing engine weight.

The mechanical design of a multiple-fan engine system has also been considered. Neglecting the more complicated transmission system, this is expected to be lighter than the other designs, and it is easier to package into an all-lifting wing airframe. Simple trade studies suggest that this can offer significant noise and fuel burn benefits provided boundary layer ingestion can be successfully implemented.

Acknowledgment

The authors are grateful to the other members of the Silent Aircraft Initiative team. Particular thanks to Matthew Sargeant, Steve Thomas, and Patrick Freuler for their input. Technical advice and assistance with the preliminary engine design software was provided by experts from Rolls-Royce plc, and the authors would like to acknowledge this contribution that made the present paper possible. This work has been financially supported by the Cambridge-MIT Institute.

Nomenclature

Symbols

- A = area
- D_f = fan tip diameter
- l = length
- $\dot{m}$ = mass flow rate
- n_{eng} = number of engine fan units in the propulsion system
- M_a = axial Mach number
- M_{rel} = relative Mach number
- N = rotational shaft speed
- p = pressure
- Q_a = fan flow capacity, $Q_a = \dot{m}\sqrt{c_p T_{02}}/A_f p_{02}$
- T = temperature
- U_{tip} = fan rotor blade tip speed
- W = weight
- X_N = net thrust
- η_f = fan isentropic efficiency

Subscripts

- 0 = total, stagnation value
- 1 = conditions at engine inlet entry
- 13 = conditions at fan exit (bypass stream)
- 2 = conditions at the engine face
- 3 = conditions at compressor exit
- 8 = condition at the nozzle exit
- eng = engine parameter
- f = fan parameter

Abbreviations

- BLD = boundary layer diversion
- BLI = boundary layer ingestion
- BPR = engine bypass ratio
- CFD = computational fluid dynamics
- FPR = fan total pressure ratio (p_{013}/p_{02})
- HPC = high pressure compressor
- IPC = intermediate pressure compressor
- LP = low pressure compressor
- MTOW = maximum take-off weight of aircraft
- OPR = overall core cycle pressure ratio (p_{03}/p_{02})
- SFC = thrust specific fuel consumption
- TET = turbine entry temperature (T_{04})
- UHBR = ultrahigh bypass ratio

References

[1] ACARE, 2000, "European Aeronautics: A Vision for 2020," Advisory Council for Aeronautics Research in Europe.

[2] Hall, C., and Crichton, D., 2005, "Engine And Installation Configurations For A Silent Aircraft, ISABE-2005–1164," presented at International Symposium on Air Breathing Engines, Munich, Germany.

[3] Crichton, D., Tan, D., and Hall, C., 2004, "Required Jet Area for a silent aircraft at take-off," presented at 8th ASC-CEAS Workshop, Budapest University of Technology and Economics, Hungary.

[4] Agarwal, A., and Dowling, A. P., 2005, "Low Freqency Acoustic Shielding of Engine Noise by the Silent Aircraft Airframe, AIAA 2005–2996," presented at 11th AIAA/CEAS Aeroacoustics Conference, Monterey, California.

[5] Gliebe, P. R., and Janardan, B. A., 2003, "Ultra-High Bypass Engine Aeroacoustic Study," NASA-2003-212525, Oct.

[6] Daggett, D. L., Brown, S. T., and Kawai, R. T., 2003, "Ultra-Efficient Engine Diameter Study," NASA CR-2003-212309.

[7] Borradaile, J. A., 1998, "Towards the Optimum Ducted UHBR Engine," Paper No. AIAA-88–2954.

[8] Crow, D. E., 2001, "A Comprehensive Approach to Engine Noise Reduction Technology," Paper No. ISABE-2001.

[9] Manneville, A., Pilczer, D., and Spakovszky, Z., 2004, "Noise Reduction Assessments and Preliminary Design Implications for a Functionally-Silent Aircraft.," presented at 10th AIAA/CEAS Aeroacoustics Conference, Manchester, UK.

[10] Liebeck, R., 2004, "Design of the Blended Wing Body Subsonic Transport," J. Aircr., **41**, pp. 10–25.

[11] The Silent Aircraft Initiative, "Silent Aircraft Initiative … A New Approach," http://silentaircraft.org.

[12] Diedrich, A., Hileman, J., Tan, D., Willcox, K., and Spakovszky, Z., 2006, "Multidisciplinary Design and Optimization of the Silent Aircraft," Paper No. AIAA 2006-1323.

[13] Berglund, B., Lindvall, T., and Schwela, D. H., 1999, "Guidelines for Community Noise," World Health Organization.

[14] "Noise Mapping England: The London Road Traffic Noise Map," 2004, Department for Environment, Food and Rural Affairs (Defra), London.

[15] Anabtawi, A. J., Blackwelder, R. F., Lissaman, P. B. S., and Liebeck, R. H., 2001, "An Experimental Study of Vortex Generators in Boundary Layer Ingesting Diffusers With a Centerline Offset," University of Southern California, Los Angeles, CA.

[16] Berrier, B. L., and Allan, B. G., 2004, "Experimental and Computational Evaluation of Flush-Mounted, S-Duct Inlets," Paper No. AIAA 2004-0764.

[17] Freuler, P., 2004, "Boundary Layer Ingesting Inlet Design for a Silent Aircraft," Master's thesis, Massachusetts Institute of Technology, Cambridge, MA.

[18] Kurzke, J., 2004, "Gas Turbine 10: A Program for Gas Turbine Performance Calculations."

[19] Crichton, D., Xu, L., and Hall, C. A., 2006, "Preliminary Fan Design for a Silent Aircraft," Paper No. GT2006-90564.

[20] Freeman, C., and Cumpsty, N. A., 1992, "Method for the Prediction of Supersonic Compressor Blade Performance," J. Propul. Power, **8**, pp. 199–206.

[21] Stone, J. R. and Montegani, F. J., 1980, "An Improved Prediction Method for the Noise Generated in Flight by Circular Jets," Paper No. NASA TM-81470.

[22] Engineering Science and Data Unit, 2003, "ESDU 98008: Prediction of Noise Generated by Fans and Compressors in Turbojet and Turbofan Engines," ESDU International Plc, London.